



Calhoun: The NPS Institutional Archive
DSpace Repository

Theses and Dissertations

Thesis and Dissertation Collection

1976

An analysis of coherent anti-stokes Raman spectroscopy as an analytical tool.

Turner, Ronald David

Monterey, California. Naval Postgraduate School

<http://hdl.handle.net/10945/17657>

Downloaded from NPS Archive: Calhoun



Calhoun is a project of the Dudley Knox Library at NPS, furthering the precepts and goals of open government and government transparency. All information contained herein has been approved for release by the NPS Public Affairs Officer.

Dudley Knox Library / Naval Postgraduate School
411 Dyer Road / 1 University Circle
Monterey, California USA 93943

<http://www.nps.edu/library>

NAVAL POSTGRADUATE SCHOOL

Monterey, California



THESIS

AN ANALYSIS OF COHERENT ANTI-STOKES
RAMAN SPECTROSCOPY AS AN ANALYTICAL TOOL

by

Ronald David Turner

June 1976

Thesis Advisor:

W. M. Tolles

Approved for public release; distribution unlimited.

T175013

REPORT DOCUMENTATION PAGE		READ INSTRUCTIONS BEFORE COMPLETING FORM
1. REPORT NUMBER	2. GOVT ACCESSION NO.	3. RECIPIENT'S CATALOG NUMBER
4. TITLE (and Subtitle) An Analysis of Coherent Anti-Stokes Raman Spectroscopy as an Analytical Tool		5. TYPE OF REPORT & PERIOD COVERED Master's Thesis June 1976
7. AUTHOR(s) Ronald David Turner		6. PERFORMING ORG. REPORT NUMBER
9. PERFORMING ORGANIZATION NAME AND ADDRESS Naval Postgraduate School Monterey, CA 93940		8. CONTRACT OR GRANT NUMBER(s)
11. CONTROLLING OFFICE NAME AND ADDRESS Naval Postgraduate School Monterey, CA 93940		10. PROGRAM ELEMENT, PROJECT, TASK AREA & WORK UNIT NUMBERS
14. MONITORING AGENCY NAME & ADDRESS (if different from Controlling Office) Naval Postgraduate School Monterey, CA 93940		12. REPORT DATE June 1976
		13. NUMBER OF PAGES 67
		15. SECURITY CLASS. (of this report) UNCLASSIFIED
		15a. DECLASSIFICATION/DOWNGRADING SCHEDULE
16. DISTRIBUTION STATEMENT (of this Report) Approved for public release; distribution unlimited.		
17. DISTRIBUTION STATEMENT (of the abstract entered in Block 20, if different from Report)		
18. SUPPLEMENTARY NOTES		
19. KEY WORDS (Continue on reverse side if necessary and identify by block number)		
20. ABSTRACT (Continue on reverse side if necessary and identify by block number) Coherent Anti-Stokes Raman Spectroscopy (CARS) is a new type of Raman Spectroscopy. The phenomenon is associated with the nonlinear conversion of two laser beams in a medium into a third collimated beam at the anti-Stokes frequency of the medium. This analysis evaluates the performance capabilities of CARS under various experimental conditions for the molecules O ₂ , N ₂ , H ₂ and CO. Laser intensity fluctuations and shot noise are		

introduced as noise sources to predict signal-to-noise ratios (S/N). The S/N is evaluated as a function of the partial pressure of a gas to measure the performance of CARS. An analysis of the uncertainty in measuring the rotational temperature is presented for diatomic gases. Inverse bremsstrahlung in plasmas is investigated as a possible process by which the parameters measured by CARS might be altered. An experiment is discussed in which an attempt was made to remove the background signal inherent in most CARS experiments. Partial interferometric cancellation of two CARS signals was observed by the proper positioning of two sample cells in an otherwise standard CARS experiment.

An Analysis of Coherent Anti-Stokes
Raman Spectroscopy as an Analytical Tool

by

Ronald David Turner
Lieutenant, United States Navy
B.S., Auburn University, 1969

Submitted in partial fulfillment of the
requirements for the degree of

MASTER OF SCIENCE IN PHYSICS

from the

NAVAL POSTGRADUATE SCHOOL
June 1976

ABSTRACT

Coherent Anti-Stokes Raman Spectroscopy (CARS) is a new type of Raman Spectroscopy. The phenomenon is associated with the nonlinear conversion of two laser beams in a medium into a third collimated beam at the anti-Stokes frequency of the medium. This analysis evaluates the performance capabilities of CARS under various experimental conditions for the molecules O_2 , N_2 , H_2 and CO. Laser intensity fluctuations and shot noise are introduced as noise sources to predict signal-to-noise ratios (S/N). The S/N is evaluated as a function of the partial pressure of a gas to measure the performance of CARS. An analysis of the uncertainty in measuring the rotational temperature is presented for diatomic gases. Inverse bremsstrahlung in plasmas is investigated as a possible process by which the parameters measured by CARS might be altered. An experiment is discussed in which an attempt was made to remove the background signal inherent in most CARS experiments. Partial interferometric cancellation of two CARS signals was observed by the proper positioning of two sample cells in an otherwise standard CARS experiment.

ACKNOWLEDGEMENTS

The author would like to express his appreciation to Professor William M. Tolles for his continuous guidance and assistance in this project. A special word of thanks goes to Dr. Gary Klauminzer of Molelectron Corporation for his interest in the project and for the use of Molelectron's facilities.

TABLE OF CONTENTS

I.	INTRODUCTION-----	7
II.	NATURE OF THE PROBLEM-----	10
	A. BACKGROUND-----	11
	B. NONLINEAR EFFECTS IN ISOTROPIC MEDIA-----	11
III.	NUMERICAL ESTIMATION OF $\chi^{(3)}$ -----	15
	A. RESONANT SUSCEPTIBILITY-----	15
	1. Cross Section-----	15
	2. Linewidths-----	16
	3. Rotational Transition Frequencies-----	16
	4. Nuclear Spin Weighting Factor-----	17
	5. Computer Program-----	17
	B. NONRESONANT SUSCEPTIBILITY-----	18
IV.	STATISTICAL CONSIDERATIONS-----	24
V.	CARS IN A PLASMA-----	30
VI.	BACKGROUND SUPPRESSION EXPERIMENT-----	34
VII.	RESULTS AND DISCUSSION-----	40
VIII.	CONCLUSIONS-----	45
	APPENDIX A: STIMULATED RAMAN SCATTERING-----	47
	COMPUTER PROGRAMS-----	55
	LIST OF REFERENCES-----	64
	INITIAL DISTRIBUTION LIST-----	67

I. INTRODUCTION

Coherent Anti-Stokes Raman Spectroscopy (CARS) is a method of chemical analysis yielding molecular spectroscopic information by utilizing nonlinear scattering phenomena. As a part of the growing field of nonlinear optics, CARS has been used to measure nonlinear coefficients in solids, liquids, and gases [1-14]. Much of today's efforts are focused on the use of CARS as a nonreactive probe in environments not conducive to other techniques for spectral analysis [14].

The intent of this thesis is to assess the usefulness of CARS as an analytical tool using the example of diatomic gases. CARS is related to the more basic phenomenon of Raman Scattering (RS). Raman scattering involves a shift in the frequency of a small portion of the photons incident on a Raman active medium. RS has been utilized extensively to obtain molecular spectroscopic information. CARS yields the same type information as RS except that the collimated CARS signal is much easier to detect.

CARS was feasible for chemical analysis only after the advent of tunable lasers of moderately high power. The initial work with CARS was performed by Maker and Terhune [15] in 1963, but only recently has the field begun to expand rapidly, as evidenced by the large number of published articles. To perform CARS in gases requires lasers of much higher power than in liquids and solids. Typically, pulsed lasers on the order of megawatts are used.

The use of such high power pulsed lasers has an inherent problem in that the power output from pulse to pulse is not constant. This introduces a source of noise that hinders the observation of weak resonances. In addition, in a mixture of gases, a CARS signal from other than the gas of interest is present as a background signal. These two factors represent at present a source of interference in observing weak molecular resonances.

As an analytical tool CARS can yield information about molecular identity, concentration and rotational temperature. Numerical estimates for the performance capabilities of CARS are based on the ability to calculate the third-order nonlinear dielectric susceptibility, $\chi^{(3)}$. This susceptibility is composed of a resonant term, χ_R , and a nonresonant term, χ_{NR} . χ_R is calculable from the physical equations that define it but χ_{NR} was deduced from experimental observations.

One source of observations for χ_{NR} relied on results from an experiment involving Stimulated Raman Scattering (SRS). Appendix A contains a development of the equations related to SRS and shows the relationship of the SRS gain equation to CARS.

A particularly difficult environment to perform conventional spectral analysis with Raman scattering is in an ionized gas called a plasma. CARS is being used in plasmas and is producing better results than conventional Raman scattering techniques. An analysis is made to predict the extent of interaction between a plasma and the laser used for a CARS experiment in the plasma. In particular, the inverse

bremsstrahlung process for the transfer of energy is analyzed.

An experimental attempt was made to improve the basic CARS experiment by the elimination of the background signal. A description of the experiment and the results are included in this study.

II. NATURE OF THE PROBLEM

The intent of this study was to theoretically investigate the analytical capabilities of CARS. The only area investigated was concerned with diatomic gases. It was desirable to estimate how small a concentration of gas could be detected and with what accuracy the rotational temperature could be measured. CARS has demonstrated its usefulness as a tool for spectral analysis. It offers orders of magnitude greater sensitivity than Raman scattering for low pressure gases. [16]

Typically, CARS experiments are performed by focusing two pulsed laser beams of different frequencies into a sample cell. The beams cross at an angle that corresponds to the momentum conservation requirement. For gases this angle is sufficiently small that the experiment may be performed with the beams colinear. One of the lasers is tunable so that the difference in the frequency of the two may be changed. When the difference in the frequency becomes close to an appropriate natural molecular frequency, the CARS signal increases markedly in amplitude.

The intensity of the CARS signal is dependent on the product of the square of the intensity of one beam and the first power of the intensity of the other. Any amplitude instability in the beams leads to amplitude instability in the CARS signal. Also, the presence of an undesirable background signal masks very small signals of interest.

A brief sketch of several publications in the field of CARS has been included in this section of the study. The basic equations related to CARS have also been included to develop the framework on which the numerical calculations were based.

A. BACKGROUND

Maker and Terhune [15], in 1963, were the first to perform a CARS experiment. Prior to the development of good tunable laser sources most of the work with CARS was developed in order to measure nonlinear coefficients of materials.

Yablonovitch, Bloembergen and Wynne [17] were among the first to use a tunable laser to generate a continuously tunable difference frequency. They investigated solid state materials such as InSb and GaAs. Levenson, Flytzanis and Bloembergen [1] followed closely with an experiment in diamond to measure the variations in $\chi^{(3)}$ as a function of the difference frequency. DeMartini [7] utilized CARS with H_2 gas in 1972 and Taran [4] in 1973 reported that he had used CARS as a means of determining the spatial distribution of H_2 gas in a flame. Taran's recent work has resulted in the spectra of several gases, temperature measurements and spatial distributions of gases in flames [14].

B. NONLINEAR EFFECTS IN ISOTROPIC MEDIA

Due to the nonlinear dielectric property of materials two laser beams may be mixed in a medium to generate a third coherent beam such that

$$\omega_3 = 2\omega_1 - \omega_2 \quad (1)$$

where ω_3 is the anti-Stokes frequency generated from the pump and Stokes frequency (ω_1 and ω_2 respectively).

The polarization vector associated with a material may be expressed as a power series:

$$P(\omega) = \chi_{(\omega)}^{(1)} \vec{E}(\omega) + \chi_{(\omega)}^{(2)} \vec{E}_{(\omega)}^2 + \chi_{(\omega)}^{(3)} \vec{E}_{(\omega)}^3 + \dots \quad (2)$$

where $\chi^{(i)}$ is the dielectric susceptibility tensor of rank $i+1$ and \vec{E} is the applied electric field. The second order term $\chi^{(2)}$ is equal to zero for isotropic liquids and gases because of inversion symmetry. The lowest order term that is present in a gas is therefore $\chi^{(3)}$, the third-order nonlinear susceptibility. There are several physical processes that involve the third order term, e.g., $3\omega_1 \rightarrow \omega_3$, $2\omega_1 + \omega_2 \rightarrow \omega_3$, $2\omega_1 - \omega_2 \rightarrow \omega_3$, etc. The last process, $2\omega_1 - \omega_2$, is the process referred to as CARS.

By assuming all fields are along one axis the components of the tensor, χ , and the electric field vector may be treated as scalars. The magnitude of the electric field may be expressed as:

$$E_i(\omega) = \frac{1}{2} [\epsilon_i e^{i(k_i z - \omega_i t)} + \text{c.c.}] \quad (3)$$

where ϵ_i is the amplitude, k_i is the propagation constant (equal to $\omega_i n_i / c$), z is the length along the z axis and t is time in seconds. For the CARS process the term E^3 in equation (2) includes $3E_1^2 E_2$ [18]. The other terms are not associated with CARS.

The resulting third order polarization, $P^{(3)}$ is given by:

$$P^{(3)} = \frac{1}{8} \left[3\chi^{(3)}(-\omega_3, \omega_1, \omega_1, -\omega_2) \right] \cdot \left[\epsilon_1^2 \epsilon_2^* e^{i[(2k_1 - k_2)z - (2\omega_1 - \omega_2)t]} + \text{c.c.} \right]. \quad (4)$$

The factor of 3 has been a point of inconsistency among authors in the past. The notation for $\chi^{(3)}(-\omega_a, \omega_b, \omega_c, \omega_d)$ is consistent with that of Bloembergen [19] for the process

$$\omega_a = \omega_b + \omega_c + \omega_d. \quad (5)$$

Solving Maxwell's equations for plane waves with polarization $P^{(3)}$ the anti-Stokes gain equation is:

$$\frac{d\epsilon_3}{dz} = \frac{i\pi\omega_3}{2c\eta_3} \epsilon_1^2 \epsilon_2^* (3\chi^{(3)}) e^{i(2k_1 - k_2 - k_3)z}. \quad (6)$$

In terms of intensity, where $I_i = \frac{c}{8\pi} |\epsilon_i|^2$, after integrating equation (6) over a length L , the result is

$$I_3 = \left(\frac{4\pi^2\omega_3}{\eta_3 c^2} \right)^2 |3\chi^{(3)}|^2 I_1^2 I_2 L^2 \left[\frac{\sin(\frac{\Delta k L}{z})}{\Delta k L / z} \right]^2 \quad (7)$$

where $\Delta k = 2k_1 - k_2 - k_3$. The conversion efficiency is defined as $\frac{P_3}{P_2}$ and if $\Delta k = 0$ the conversion efficiency becomes a maximum. Because of the small dispersion of light in gas, CARS may be performed with ω_1 , ω_2 and ω_3 colinear. For a focused beam (assumed to be a cylinder of plane waves and $\Delta k = 0$) the conversion efficiency becomes:

$$\frac{P_3}{P_2} = \epsilon = \left(\frac{2}{\lambda_1} \right)^2 \left(\frac{4\pi^2 \omega_3}{n_3 c^2} \right)^2 \left| 3\chi^{(3)} \right|^2 P_1^2. \quad (8)$$

The third order nonlinear dielectric susceptibility, $\chi^{(3)}$, is composed of a frequency dependent resonant part (χ_R) and a nearly frequency independent part, the nonresonant susceptibility, χ_{NR} :

$$\chi^{(3)} = \chi_R + \chi_{NR}. \quad (9)$$

χ_R can be expressed [18] as:

$$\chi_R = \frac{2Nc^4}{3\hbar\omega_2^4} \frac{d\sigma}{d\Omega} \frac{\Delta \omega_v}{[\omega_v^2 - (\omega_1 - \omega_2)^2 - i\gamma(\omega_1 - \omega_2)]}. \quad (10)$$

When $\omega_1 - \omega_2 = \omega_v$, the resonant susceptibility becomes

$$\chi_R = \frac{2Nc^4}{3\hbar\omega_2^4} \frac{d\sigma}{d\Omega} \Delta \frac{i}{\gamma} \quad (11)$$

where N is the number density of molecules, $(\frac{d\sigma}{d\Omega})$ is the Raman cross section for scattering, Δ is the difference in probability of finding a molecule in the ground and first vibrational states, and γ is the line width, full width at half-maximum intensity.

III. NUMERICAL ESTIMATION OF $\chi^{(3)}$

As defined in Section II.B., $\chi^{(3)}$ is composed of two parts, the resonant and nonresonant susceptibility. The resonant part is associated with the various Raman active frequencies that characterize a molecule. The equation for χ_R has been derived [18] from considerations of a driven harmonic oscillator and quantum mechanics. χ_{NR} is associated with the electronic structure of the molecule and is nearly frequency independent.

Equation (10) defines χ_R in terms of an entire vibrational band, namely the ground state. To estimate χ_R for each rotational level requires an analysis of each of the terms in equation (10) that are functions of the rotational quantum number J . As will be shown in Section IV, the signal-to-noise ratio for a CARS experiment is a function of the peak value of χ_R . Being able to predict signal-to-noise ratios is important when deciding which analytical technique to employ for a certain situation. Due to the complexity of the calculations a computer program was utilized to predict the peak value of χ_R for several gases.

A. RESONANT SUSCEPTIBILITY, χ_R

1. Cross Section

The Raman cross section for scattering is typically quoted as the cross section for an entire vibrational band. For computational purposes it was necessary to apportion this

total value among the rotational levels. The relative population of a rotational level was used as the apportioning factor such that

$$\left(\frac{d\sigma}{d\Omega}\right)_J = g_J \frac{(2J+1) \exp[-BJ(J+1)/kT]}{Q} \left(\frac{d\sigma}{d\Omega}\right)_{\text{Total}}, \quad (12)$$

where

$$Q = \sum_J g_J (2J+1) \exp[-BJ(J+1)/kT],$$

J is the rotational quantum number, g_J is the nuclear spin weighting factor and B is the rotational constant. The values used for $\frac{d\sigma}{d\Omega}$ were from Chang [20]. His measurements of cross section were the results of experiments using a ruby laser at 5140\AA . The cross section has a fourth power frequency dependence (ω^4) thus an accurate calculation of χ_R requires that the data be corrected for this factor.

2. Linewidths

On resonance the CARS signal is proportional to the inverse square of the linewidth. Two general extremes of linewidth were used, the Doppler broadened and collision broadened cases. The Doppler broadened lines are narrower than the collision (or pressure) broadened lines.

3. Rotational Transition Frequencies

For molecules that exhibit Raman active vibrational and rotational frequencies the CARS signal increases in amplitude as the difference frequency approaches one of the molecular resonance frequencies. The rotational frequency for a vibration-rotation transition of a diatomic molecule is expressed as:

$$\omega_{v,J} = \omega_e - 2\omega_e x_e (v + 1) - \alpha_e J(J + 1) \quad (13)$$

where ω_e is the harmonic vibrational angular frequency, x_e is the anharmonic constant, v and J are the quantum numbers of vibration and rotation respectively, and α_e is the rotation-vibration interaction constant.

4. Nuclear Spin Weighting Factor

Homonuclear diatomic gas molecules have a statistical correction factor for the population of rotational levels due to the spin of each of the nuclei. Alternating lines in the rotational spectra have intensity ratios $1:(I/I+1)$ where I is the spin of each nucleus. The strong line of D_2, O_2 and N_2 are the even numbered J levels while H_2 's strong lines are associated with odd numbered J levels. TABLE 1 summarizes the degeneracy weighting factor, g_J .

TABLE 1

NUCLEAR SPIN WEIGHTING FACTORS (g_J)

Gas	Nuclear Spin (I)	g_J for Even # J Levels	g_J for Odd # J Levels
<u>O₂</u>	<u>0</u>	<u>1</u>	<u>0</u>
<u>H₂</u>	<u>1/2</u>	<u>1/3</u>	<u>1</u>
<u>N₂</u>	<u>1</u>	<u>1</u>	<u>1/2</u>

Note that CO is not a homonuclear molecule and thus has no degeneracy factor; i.e., $g_J = 1$ for all J .

5. Computer Program

To calculate χ_R as a nearly continuous function of the difference frequency required a computer program. A

Fortran program was written (See page 54) to calculate the maximum amplitude of χ_R as a function of the difference frequency according to the following equation:

$$\chi_{R, (\omega_1 - \omega_2)} = \frac{2Nc^4}{3\hbar\omega_2^4} \frac{d\sigma}{d\Omega} \frac{\Delta}{Q} \sum_J \frac{[g_J(2J+1)e^{-BJ(J+1)/kt}]_{\omega_{v,J}}}{\omega_{v,J}^2 - (\omega_1 - \omega_2)^2 - i\gamma(\omega_1 - \omega_2)} . \quad (14)$$

Tables 2 and 3 give the results of the computations.

B. NONRESONANT SUSCEPTIBILITY χ_{NR}

In 1967 Rado [21] performed a series of experiments to measure the magnitude of the nonresonant susceptibility, χ_{NR} , of several gases. The impetus for the experiments was to measure the peak resonant anti-Stokes power from a hydrogen cell and compare that to the nonresonant anti-Stokes power generated in a sample cell. The ratio of powers would be equal to the square of the ratio of the susceptibilities:

$$\frac{P_{\text{sample}}}{P_{H_2}} \propto \frac{(\chi_{NR}^{\text{(Sample)}})^2}{(\chi_P^{(H_2)})^2} . \quad (15)$$

The value Rado chose to use for χ_P was from an earlier work with phonon lifetimes and SRS gain coefficients. The relationship of χ_P and the SRS gain coefficient is discussed in Appendix A. His calculated value of χ_{NR} for N_2 is $1.35 \times 10^{-18} \frac{\text{cm}^3}{\text{erg}}$. Based on Table 3, χ_P for N_2 at 300 K is $2.4 \times 10^{-16} \frac{\text{cm}^3}{\text{erg}}$. Thus, the ratio of the peak to nonresonant susceptibilities is

TABLE 2

<u>Gas</u>	<u>Linewidth (cm^{-1})</u>	<u>Temp ($^{\circ}\text{K}$)</u>	<u>$\chi_p (\text{cm}^3/\text{erg})$</u>
O_2	<u>.0034</u>	<u>300</u>	<u>8.3×10^{-15}</u>
	<u>.0076</u>	<u>1500</u>	<u>2.0×10^{-16}</u>
N_2	<u>.0055</u>	<u>300</u>	<u>3.3×10^{-15}</u>
	<u>.012</u>	<u>1500</u>	<u>1.1×10^{-16}</u>
H_2	<u>.036</u>	<u>300</u>	<u>1.0×10^{-14}</u>
	<u>.07</u>	<u>1500</u>	<u>4.3×10^{-16}</u>
CO	<u>.005</u>	<u>300</u>	<u>3.3×10^{-15}</u>
	<u>.07</u>	<u>1500</u>	<u>2.2×10^{-17}</u>

TABLE 3

<u>Gas</u>	<u>Linewidth (cm^{-1})</u>	<u>Temp ($^{\circ}\text{K}$)</u>	<u>$\chi_p (\text{cm}^3/\text{erg})$</u>
O_2	<u>.16</u>	<u>300</u>	<u>2.6×10^{-16}</u>
	<u>.07</u>	<u>1500</u>	<u>2.5×10^{-17}</u>
N_2	<u>.14</u>	<u>300</u>	<u>2.4×10^{-16}</u>
	<u>.06</u>	<u>1500</u>	<u>2.6×10^{-17}</u>
H_2	<u>.03</u>	<u>300</u>	<u>1.2×10^{-14}</u>
	<u>.08</u>	<u>1500</u>	<u>4.0×10^{-16}</u>
CO	<u>.15</u>	<u>300</u>	<u>2.6×10^{-16}</u>
	<u>.011</u>	<u>1500</u>	<u>1.1×10^{-16}</u>

$$\frac{\chi_P}{\chi_{NR}} \simeq 178.$$

An independent method to estimate the magnitude of χ_{NR} was provided by the spectra of N_2 published by Taran [14]. For the unresolved spectra the difference in frequency of the maximum and minimum values of the CARS signal, $\delta\omega$, is given by the relation

$$\delta\omega = \gamma \left(1 + \frac{\chi_P^2}{4\chi_{NR}^2} \right)^{\frac{1}{2}}. \quad (16)$$

Assuming a linewidth of 1.8 cm^{-1} and a $\delta\omega$ of 42 cm^{-1} the calculated result is that

$$\left(\frac{\chi_P}{\chi_{NR}} \right)_{N_2} \simeq 47. \quad (17)$$

By estimating the level of the background signal in the N_2 spectrum, another ratio of χ_P/χ_{NR} is equal to

$$\left(\frac{\chi_P}{\chi_{NR}} \right)_{N_2} \simeq 75. \quad (18)$$

Knowing the peak value of χ_R yields an estimate of χ_{NR} .

An earlier work by Taran [4] provides another means of estimating the ratio of the susceptibilities. The total pressure of a H_2, N_2 mixture was maintained at one atmosphere. The anti-Stokes intensity generated was plotted as a function of the H_2 concentration.

If χ_R and χ_{NR} scale linearly with pressure, then the total susceptibility of the mixture may be approximated by

$$\chi^{(3)} = \chi_R P + [1-P]\chi_{NR} \quad (19)$$

where P is the partial pressure of H_2 . As a ratio of χ_R to χ_{NR} the observed anti-Stokes power is approximated by

$$I_3 \propto |\chi^{(3)}|^2 \simeq \chi_{NR}^2 \left[\left[\frac{\chi_R}{\chi_{NR}} - 1 \right] P^2 + 1 \right]^2. \quad (20)$$

When the log of intensity is plotted against the log of P (See Figure 1), the predicted and observed curves are in fair agreement for a ratio of $10^4:1$. That is

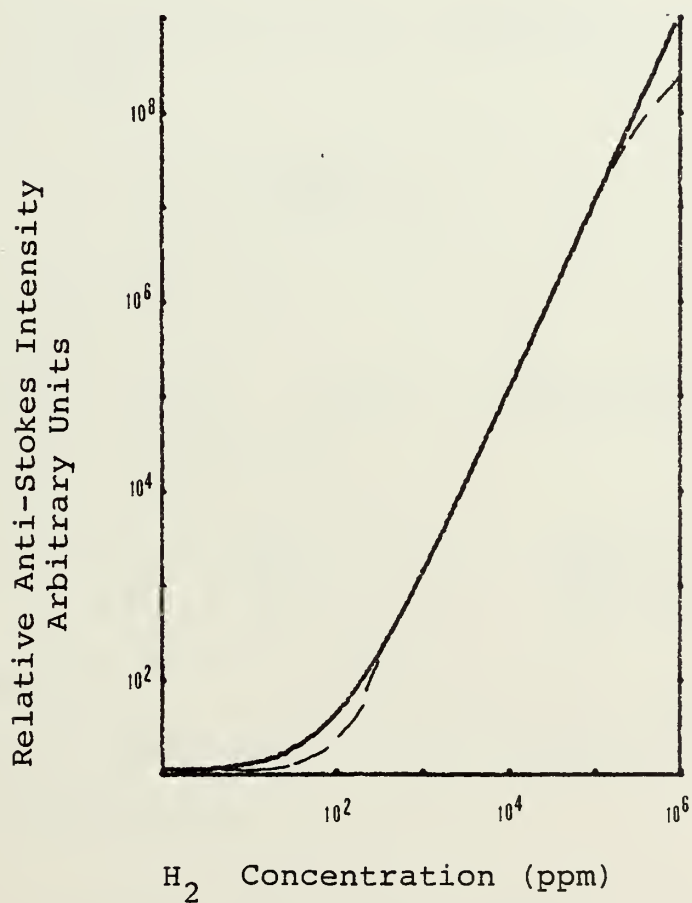
$$\frac{\chi_R^{(H_2)}}{\chi_{NR}^{(N_2)}} \simeq 10^4. \quad (21)$$

Based on the analysis of the H_2, N_2 plot and using the value of χ_P for H_2 from Table 3, the value of χ_{NR} for N_2 is estimated to be $1.2 \times 10^{-18} \frac{\text{cm}^3}{\text{erg}}$. Thus, another estimate of the ratio is

$$\frac{\chi_P}{\chi_{NR}} = \frac{2.4 \times 10^{-16}}{1.2 \times 10^{-18}} \simeq 200.$$

The factor of four between the high and low estimates of the ratio is not surprising based on the variety of sources used to estimate them.

Figure 1. Taran's results follow dotted line. The solid line is the predicted curve for $\frac{\chi_R}{\chi_{NR}} = 10^4$. The two curves are equal from 10^3 to 10^5 ppm.



IV. STATISTICAL CONSIDERATIONS

The anti-Stokes power resulting from a tightly focused CARS experiment is expressed as [18]:

$$P_3 \approx K \left| \chi^{(3)} \right|^2 P_1^2 P_2 \quad (22)$$

where

$$K = \left(\frac{2}{\lambda_1} \right)^2 \frac{4\pi^2 \omega_3^2}{\eta_3 c^2} \quad (23)$$

The resonant susceptibility may be expressed in terms of its peak value, χ_p , by:

$$\chi_R = \frac{\chi_p \gamma}{2\Delta\omega - i\gamma} \quad (24)$$

where $\Delta\omega = \omega_1 - \omega_2 - \omega_v$.

For weak signals in which $\chi_p \ll \chi_{NR}$, the absolute value squared of $\chi^{(3)}$ is given by

$$\left| \chi^{(3)} \right|^2 = \left| \chi_{NR} + \frac{\chi_p \gamma}{2\Delta\omega - i\gamma} \right|^2 \approx \chi_{NR}^2 + \frac{2\chi_p \gamma \Delta\omega}{4(\Delta\omega)^2 + \gamma^2} \quad (25)$$

The magnitudes of $\chi^{(3)}$ at its extrema are $\chi_{NR} \pm \chi_p/2$. For a signal strength proportional to the difference in the peak and background susceptibility

$$I_3 \propto \left(\chi_{NR} + \frac{\chi_p}{2} \right)^2 \approx \chi_{NR}^2 + \chi_{NR} \chi_p \quad (26)$$

Thus, for $\chi_p \ll \chi_{NR}$, the anti-Stokes power above that due to χ_{NR} alone, is

$$P_3 \cong K \chi_{NR} \chi_P P_1^2 P_2 \eta_T \quad (27)$$

where η_T is an efficiency coefficient to take into account the optical losses, detector inefficiencies and observed conversion efficiency factor.

Typically, the largest source of noise when performing CARS on samples at one atmosphere pressure is associated with the power fluctuations of the pump and Stokes beams. If the power of the laser source, P_L , has a relative standard deviation of ϵ_p , the standard deviation of the power is $\epsilon_p P_L$. The fluctuation of the background signal power P_N , due to χ_{NR} is thus:

$$P_N \approx 3 \epsilon_p K \chi_{NR}^2 P_1^2 P_2 \eta_t \quad (28)$$

assuming each beam has the same relative standard deviation ϵ_p .

For a low intensity CARS signal in the absence of background one finds the major source of noise to be the shot noise of the signal. For an N photon signal the standard deviation is \sqrt{N} .

For a pulsed signal the noise power due to shot noise is

$$P_N^2 = \frac{P_3 h\nu}{\tau} \quad (29)$$

The signal-to-noise ratio for the background limited case given by equations (27) and (28) becomes

$$S/N \approx \frac{\chi_P}{3\epsilon_p \chi_{NR}} \quad (30)$$

whereas the signal-to-noise ratio for a situation in which there is only a very weak signal is given by equations (27)

and (29) to be

$$S/N \approx (K \chi_p^2 P_1^2 \eta_T)^{\frac{1}{2}} (\tau/h\nu)^{\frac{1}{2}}. \quad (31)$$

As an application of the signal-to-noise problem consider the measurement of χ_p from a spectral envelope. The uncertainty of χ_p , σ_p , is expressed as: [22]

$$\frac{1}{\sigma_p^2} = \sum_i \frac{1}{\sigma_i^2} \quad (32)$$

where σ_i is the standard deviation in determining σ_p from the i^{th} pulse of a pulsed laser. For CARS with a background limited situation and $\chi_p \ll \chi_{NR}$ the uncertainty in the signal amplitude is approximately a constant, σ_m , associated with the laser power fluctuations.

Thus $\sigma_i = \sigma_m \left(\frac{\partial \chi_p}{\partial I(\omega_i, J, T)} \right)$ where σ_m is basically the

noise power given by equation (28):

$$\sigma_m = 3 \epsilon_p K \chi_{NR}^2 P_1^2 P_2. \quad (33)$$

$I(\omega_i, J, T)$ is the intensity of the spectral envelope at ω_i , due to the quantum rotational number J , at temperature T .

The result of this analysis yields [16]:

$$\sigma_p = \frac{\sigma_m}{K P_1^2 \chi_{NR}} \left(\frac{2\Delta\omega}{\pi\gamma} \right)^{\frac{1}{2}} \quad (34)$$

or

$$\sigma_p = \frac{1}{S/N} \left(\frac{2\Delta\omega}{\pi\gamma} \right)^{\frac{1}{2}} \quad (35)$$

In general any standard deviation is dependent on the number of times, N , the measurement is taken such that

$$\sigma_p \propto \frac{1}{\sqrt{N}} .$$

The conclusion is that for a given S/N the term $(\frac{\pi\gamma}{2\Delta\omega})$ is the effective number of pulses required at intervals of $\Delta\omega$ to produce an uncertainty, σ_p , in the measurement of χ_p .

The uncertainty in determining the rotational temperature is a product of the nearly constant background uncertainty, σ_m , and the small change of intensity with temperature. A convenient definition for σ_m is:

$$\sigma_m = I_{\max} \delta_{I_{\max}} \quad (36)$$

where $\delta_{I_{\max}}$ is the relative uncertainty in the amplitude of the line of maximum intensity. The uncertainty in the temperature then becomes [16]:

$$\frac{1}{\sigma_T^2} = \frac{1}{\sigma_m^2} \Sigma_J \left(\frac{\partial I_{J,T}}{\partial T} \right)^2 . \quad (37)$$

The intensity of a line is proportional to the Boltzmann population distribution. The change of intensity with temperature has been shown [16] to be:

$$\frac{\partial I_{J,T}}{\partial T} = I_{J,T} \frac{[BJ(J+1) - kT]}{kT^2} . \quad (38)$$

The resultant standard deviation in temperature is

$$\sigma_T^2 = \frac{T^2 [\delta_{I_{\max}}]^2}{\sum_J \left\{ \frac{I_{J,T}}{I_{\max}} \left[\frac{BJ(J+1)}{kT} - 1 \right] \right\}^2} \quad (39)$$

It has been estimated [16] that for an uncertainty in the maximum intensity equal to 2% the temperature of CO at 1500°K may be determined to within 10°K.

This uncertainty in temperature is for an unrealistic situation in that each rotational line is completely resolved. A more realistic situation is the case of a continuous envelope as given in equation (14). A computer program (see page 59) was written to calculate the uncertainty in a temperature measurement, σ_T , based on equation (37).

$$\frac{1}{\sigma_T^2} = \frac{1}{\sigma_m^2} \sum_i \left(\frac{\partial I(\omega_i, J, T)}{\partial T} \right)^2$$

$$\sigma_m = I_p \epsilon_p = K \chi_p^2 \epsilon_p$$

$$\frac{1}{\sigma_T^2} = \frac{1}{\epsilon_p^2} \sum_i \left[\frac{1}{I_p} \frac{\partial (K \chi_p^2(\omega_i, J, T))}{\partial T} \right]^2$$

$$\frac{1}{\sigma_T^2} = \frac{1}{\epsilon_p^2} \sum_i \left[\frac{\partial \left(\frac{\chi_p^2(\omega_i, J, T)}{\chi_p^2} \right)}{\partial T} \right]^2$$

For the same conditions used to calculate the previous uncertainty in temperature the results of the envelope calculation yields an uncertainty of 15°K. This value is of the same order of magnitude as the statistical prediction of 10°K,

estimated by using equation (39). It is to be expected that the uncertainty would be higher for measurements on the spectral envelope. Verification of the statistical approach means that the much simpler method for predicting the uncertainty is a good approximation.

V. CARS IN A PLASMA

Low pressure ionized gases, or plasmas, represent a class of materials that are receiving very close investigation. The population of the various energy levels reveals much about the plasma. Determining the population of levels is a very difficult task with conventional Raman spectroscopy. CARS has been utilized to obtain spectra of several plasmas at the Naval Research Laboratory, Washington, D. C. The experience there indicates that the technique is not difficult and produces useful information.

Of importance when analyzing CARS in a plasma is how much the high power laser beams may be expected to perturb the system under investigation. The major source of interaction between the plasma and laser beams appears to be from the inverse bremsstrahlung process [23]. The free electrons in the plasma will gain kinetic energy by this process.

If the laser frequency is above the plasma frequency the light will propagate through but there will be some attenuation or absorption. The plasma frequency is given by [24]

$$\omega_P = \left(\frac{4\pi\eta_e e^2}{M_e} \right)^{\frac{1}{2}} \quad (40)$$

where η_e is the number density of electrons (cm^{-3}), e is the charge of an electron (esu) and M_e is the mass of an electron (grams).

An estimate of the change in the electron kinetic energy may be made by assuming there is an absorption coefficient, α ,

for the plasma. The energy absorbed per unit volume of the plasma is

$$E_{\text{ABS}} = \frac{I_0 (1 - e^{-\alpha x}) \Delta t A}{Ax} \approx \frac{P_0 \Delta t \alpha}{A} \quad (41)$$

where I_0 is the incident intensity, P_0 is the incident power, Δt is the pulse duration, A is the beam cross section and x is the path length of the medium. If all the absorbed energy is transferred to the kinetic energy of the electrons then the energy absorbed per electron is

$$E_{\text{ABS}} \approx \frac{\alpha P_0 \Delta t}{A n_e} \quad (42)$$

As a fraction of the initial energy, $3/2 k T_e$,

$$\frac{E_{\text{ABS}}}{3/2 k T_e} \approx \frac{\alpha P_0 \Delta t}{3/2 A n_e k T_e} \quad (43)$$

where T_e is the electron temperature. The absorption coefficient, α , for inverse bremsstrahlung has been reported as [25]

$$\alpha = 4/3 \left(\frac{\pi}{3/2 k T} \right)^{1/2} \frac{n_e n_i z^2 e^6}{h c M_e^{3/2} \nu^3} [1 - \exp(-\frac{h\nu}{kT})] \quad (44)$$

where n_i is the ion number density, z is the charge of the ions and ν is the frequency of the incident light. Evaluation of equation (43) with α defined by equation (44) results in a relative change of temperature equal to

$$\frac{\partial T_e}{T_e} = \frac{1.3 \times 10^{25} n_i z^2 P_0 \Delta t [1 - \exp(-h\nu/kT)]}{\nu^3 A (k T_e)^{3/2}} \quad (45)$$

This agrees favorably with an equation for the change of electron temperature given by [23]

$$\frac{\Delta kT_e}{kT_e} = \frac{1.4 \times 10^{25} \eta_i z^2 [1 - \exp(-h\nu/kT)] \int_0^T P_L dt}{v^3 (kT_e)^{3/2} A} \quad (46)$$

where (kT_e) is in electron volts and P_L is the power of the laser in watts.

The equipartition time, t_e , is the average time required for the electrons to transfer their excess kinetic energy to the ions and thus reach an equilibrium temperature. The equation for t_e is given by [25]

$$t_e \approx \frac{25.2 A (T_e)^{3/2}}{\eta_e z^2} \quad (47)$$

where A is the atomic weight of the ions, T_e is the electron temperature in degrees Kelvin, and η_e is in cm^{-3} . If the duration of the laser pulse is shorter than t_e then any energy the electrons gained by inverse bremsstrahlung will not be transferred to the ions and there will be very little perturbation of the molecules under investigation.

Consider the following as a typical example:

plasma: Deuterium at 50 Torr, $T_e = 10^4$ K

$\eta_e = 10^{11} \text{ cm}^{-3}$, 20 cm long

laser: 5500\AA , 5MW, 10^{-4} cm^2 beam area, 20 nsec duration

The plasma frequency, ω_p , equals $1.8 \times 10^{10} \text{ sec}^{-1}$ and $\omega_L \gg \omega_p$.

The equipartition time, t_e , equals 20 micro seconds. The

relative change in electron temperature given by equation (46) is .0001%. Little perturbation of the plasma is expected from these conditions.

VI. BACKGROUND SUPPRESSION EXPERIMENT

As discussed earlier, the nonresonant susceptibility, χ_{NR} , is responsible for the background signal. The power amplitude fluctuations of the lasers produce noise on this signal. The resonant signal above the background also has noise on it. It would be much easier to detect the resonant signal if there were no noise on the background or, better yet, no background at all. The desire for reduction of the background signal led to an idea [26] for an experiment to determine if it was possible to completely suppress the background. In addition to yielding much better signal quality the elimination of the background would limit the detectability of CARS to the limit of conversion efficiency.

Typically, the diluent of a sample provides the largest contribution to χ_{NR} . The basic idea for suppression of the background signal was to perform two CARS experiments in series. In the first experiment the generated anti-Stokes beam, ω_3 , would be due to only χ_{NR} (of a diluent) and in the other experiment the anti-Stokes beam, ω_3' , would be due to $\chi_{NR} + \chi_R$ (the sample plus the diluent). If the ω_3 beam, from the first cell, were then forced out of phase by $N\pi$ radians (where N is an odd integer) relative to the second beam, ω_3' , and superimposed on the second then the resultant signal should be only that due to χ_R of the sample.

Molelectron Corporation of Sunnyvale, California, through Dr. G. Klauminzer provided equipment, facilities and assistance for conducting the experiments.

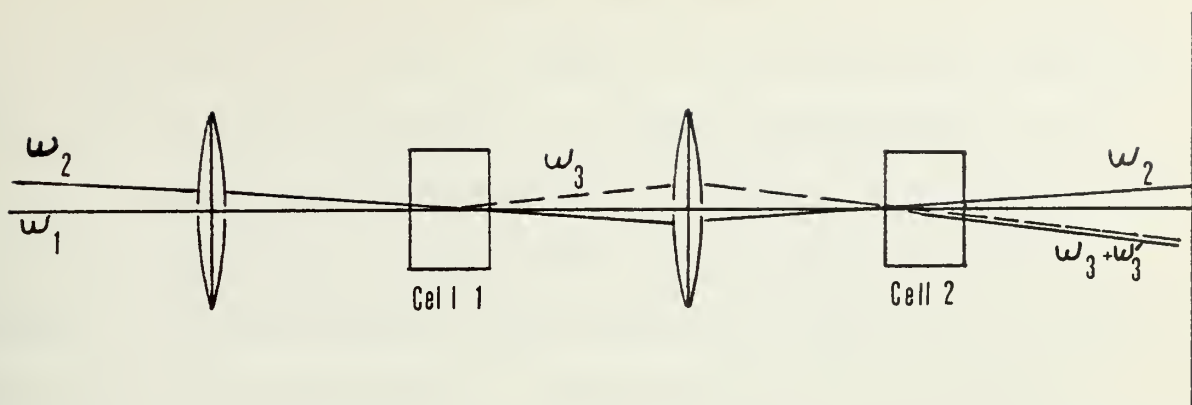


Figure 2. Arrangement of Equipment for Background Suppression Experiment.

Figure 2 shows the basic arrangement found to be most convenient. A pulsed nitrogen laser was used to drive two tunable dye lasers in an arrangement reported by Dr. Klauminzer in Reference 12.

Benzene was chosen as the first material to work with since it was known that the CARS signal was very strong and visible. For benzene the values for ω_1 , ω_2 and ω_3 were 480., 504. and 458.2 nm, respectively.

Both cells were filled with benzene in anticipation of demonstrating complete cancellation of ω_3' with ω_3 . It was known that a translation of cell one along the focal axis would change the intensity of ω_3 by changing the volume in the focal region but it was also discovered that the same translation changed the phase of ω_3 relative to ω_3' . To completely cancel ω_3' it was known that several conditions had to be met. The beam had to be π radians out of phase, the intensities had to be equal and the beams had to be coincident. A plot of the resultant intensity versus the translation

of cell one revealed that there was constructive and destructive interference of the two beams. The destructive interference was not complete though. A visual observation of the $\omega_3 + \omega_3'$ beam revealed interference fringes. By steering the ω_3 beam off of the ω_3' beam the fringe pattern could be changed. It was suspected that chromatic aberration in the focal lens was responsible. Calculation of the effect of chromatic aberration indicated that the fringe pattern should be approximately that observed. The use of an achromat for the focal lens reduced the number of fringes visible but it was found that a slight rotation of the lens changed the pattern considerably.

The best measured ratio of minimum to maximum intensity as a function of cell translation was observed to be 10:1. Since it was the electric fields that were interfering, the 10:1 ratio amounts to about a 60% cancellation factor. The cancellation factor was arrived at by considering the incomplete phase cancellation of the electric fields. The observed intensity is proportional to

$$\left| E_1 e^{i\theta_1} + E_2 e^{i\theta_2} \right|^2. \quad (48)$$

If the amplitudes E_1 and E_2 are equal, the resulting intensity is proportional to

$$E^2 (e^{i\theta_1} + e^{i\theta_2}) (e^{-i\theta_1} + e^{-i\theta_2}) \quad (49)$$

or

$$I \propto E^2 (2 + 2 \cos(\theta_1 - \theta_2)). \quad (50)$$

Complete constructive interference, when $\theta_1 = \theta_2$, results in an intensity four times that of one beam, and complete destructive interference would result in no intensity.

It is not surprising that on the average complete interference does not take place. For a small difference in θ_1 and θ_2 the observed magnitude is slightly less than $4E^2$ or slightly more than zero.

An observed 9:1 intensity ratio is equivalent to a 3.6 to .4 ratio on the normalized scale, $E^2 = 1$. Thus, the interference produces a signal equal to 40% of what one beam would produce, therefore, a cancellation factor of 60%.

Next, a three molar sodium benzoate solution was used in the cells in place of benzene. Again there was incomplete cancellation. The best observed ratio of intensities was 5:1. It had been predicted that sweeping the frequency of ω_2 to record a spectrum would not alter the phase difference of ω_3 and ω_3' . The first observations made while sweeping ω_2 revealed that ω_3 and ω_3' went in and out of phase over a period of about 10 cm^{-1} . By changing the optical path length of ω_3 or ω_1 and ω_2 by use of microscope slides the period could be increased to about 60 cm^{-1} .

The observed increase in the period of the oscillation verified that the optical path length could be controlled to shift ω_3 and ω_3' in and out of phase. With the appropriate optical path length the period of the oscillation could be adjusted to infinity.

A spectrum was recorded for the three molar sodium benzoate, two cell, series cancellation experiment. Of interest from the

spectra is the interference of the background with respect to the noise levels observed. Figure 3 is a portion of that spectrum depicting the observed resultant signal. When the interference was constructive the noise was much higher than for the destructive interference.

As stated earlier, the reason for the experiment was to increase the sensitivity of CARS. An analysis of the signal-to-noise ratio for a cancellation experiment indicates that the cancellation has to be much more effective than was observed in this experiment to gain an order of magnitude increase in the signal-to-noise ratio.

Assume b^2 is the fraction of background intensity remaining after cancellation. Then, the S/N ratio is given by

$$S/N \approx \frac{\chi_p}{3\epsilon_p (b\chi_{NR})} ,$$

similar to the development of equation (30). An increase in S/N of 10 requires $b^2 = .01$, or a 99% cancellation factor. A 400:1 intensity ratio would correspond to such a cancellation factor.

The experiment as performed was very sensitive to the alignment and quality of the optics involved. One of the major contributions to the incomplete cancellation is probably the diffraction limited ability of the center lens to perfectly image the initial ω_3 beam onto ω_3' . Other macroscopic factors such as turbulence and inhomogeneity of the samples are other obstacles to complete cancellation.

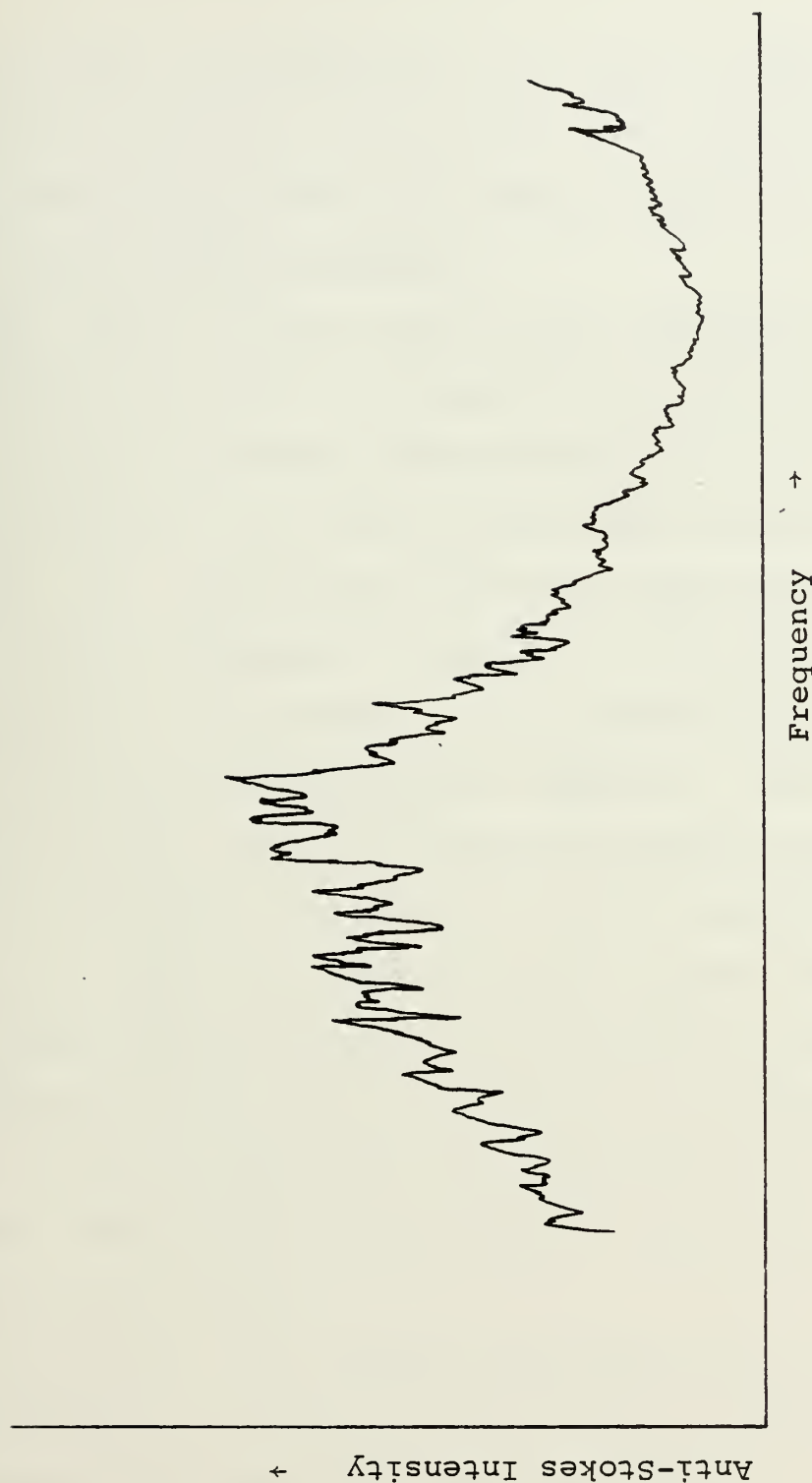


Figure 3. Portion of recorded spectrum from background suppression experiment. Depicts background signal changing from constructive to destructive interference.

VII. RESULTS AND DISCUSSION

The basis for determining the areas of application for a new analytical tool, such as CARS, must depend on recognizing the limits beyond which the technique cannot be expected to yield the desired information.

The results of this analysis are presented as lower limits of concentration that are expected to be detectable by CARS. For a mixture of gases, the detectability of one gas depends on the ratio of χ_R and χ_{NR} , the same as Taran's plot for H_2 and N_2 . Plots of the ratios for other gases with N_2 as a diluent are presented in Figure 4. The minimum detectable concentration is dependent on the required signal-to-noise ratio for a given experimental condition. The lower limit of detection for a pure gas at reduced pressures would be limited to the conversion efficiency if not for the photon statistics involved. From the signal-to-noise analysis, estimates of the detectable lower pressures are summarized in Figures 5 and 6.

Based on the results of Section IV the rotational temperature of a gas is expected to be measurable to within 1%. That assumes the amplitude fluctuations of the CARS signal observed remain less than 10%.

In a plasma, the inverse bremsstrahlung process is expected to be a relatively insignificant perturbation to the parameters determined by a CARS experiment.

The experimental attempt at cancellation of the background confirmed the idea that interferometric cancellation is a

possible technique for improving CARS when the background becomes a problem. The observed results were not of the magnitude hoped for but did serve to verify the concept and to recognize a possible source of limiting performance.

Turbulence in the samples and inhomogeneity may be part of the reason that incomplete cancellation occurs. The major contribution to the lack of complete cancellation is probably the result of diffraction limited optics. The first beam cannot be refocused through a lens and have precisely the same geometry that it had originally.

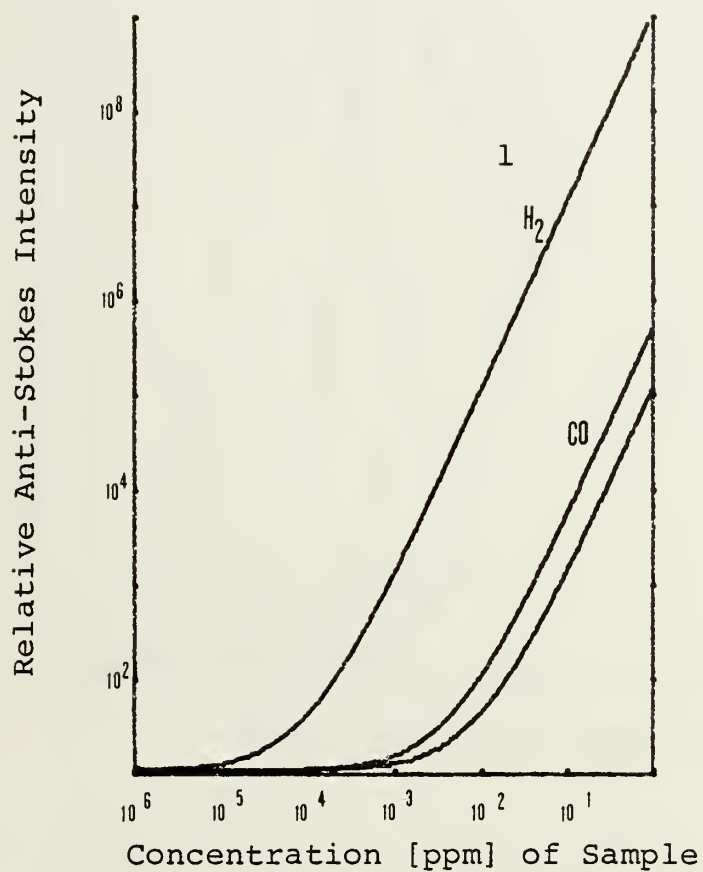


Figure 4. Log-log plots of N_2 gas mixtures at 1 atmosphere total pressure. H_2 at 300 K. Upper CO plot at 300 K, Lower coplot at 1500 K. χ_{NR} of N_2 assumed to be $1.2 \times 10^{-18} \frac{\text{cm}^3}{\text{erg}}$ at 300 K, and $.24 \times 10^{-18} \frac{\text{cm}^3}{\text{erg}}$ at 1500 K.

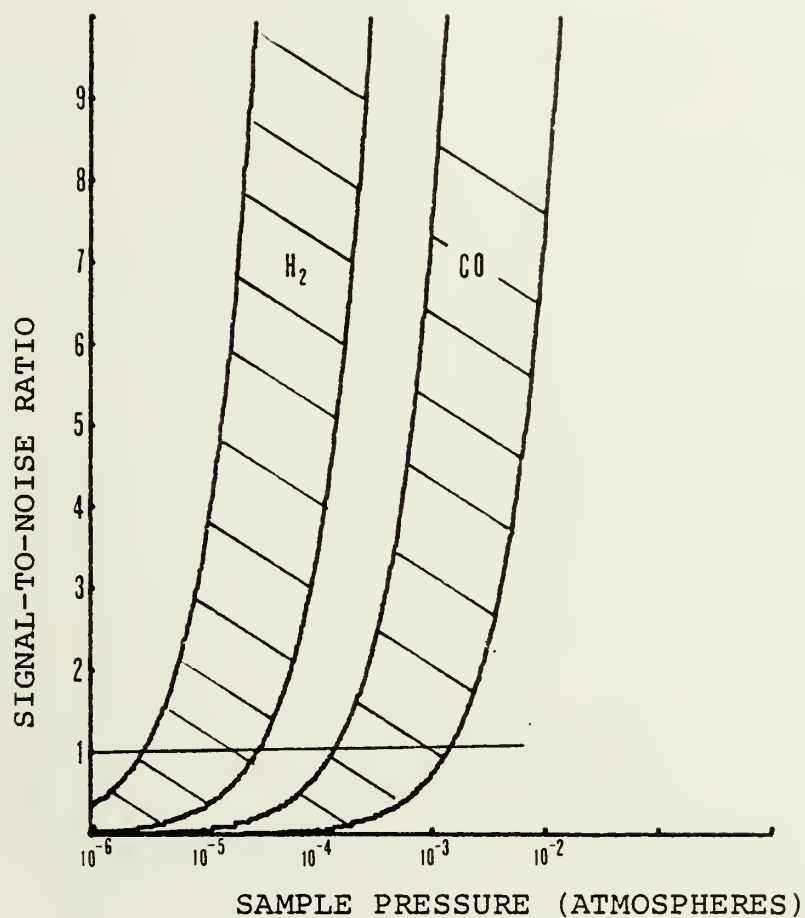


Figure 5. Signal-to-noise ratios for gas mixtures at 300 K with a total pressure of 1 atmosphere. Background pressure and signal due to N_2 . The area boundaries are defined by assuming values of the uncertainty in the pulsed laser intensity, ϵ_p , from 10^{-2} to 10^{-1} .

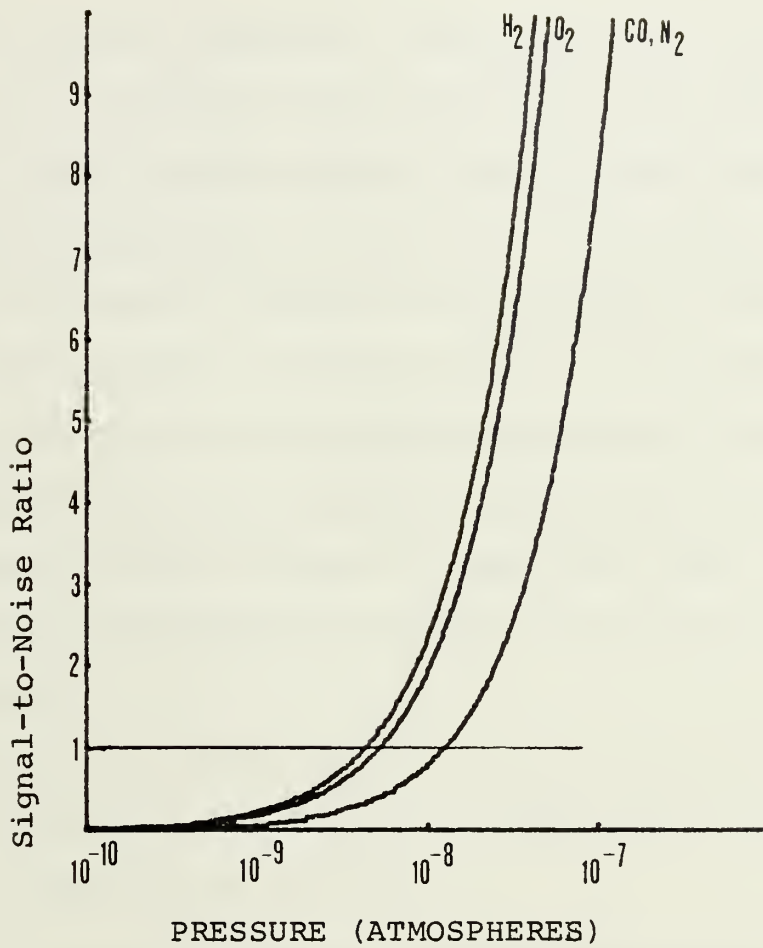


Figure 6. Signal-to-noise ratios for Doppler broadened gas at 300°K as a function of pressure. Noise due to photon statistics. The assumed parameters are
 $\eta_T = .01$, $P_1 = 5MW$, $P_2 = .5MW$, $\tau = 20$ nsec,
 $\lambda = 5500 \text{ \AA}$.

VIII. CONCLUSIONS

This analysis presents a model by which the limits of the information available from CARS may be predicted. At STP typical diatomic gases should have a signal-to-noise ratio of 1 at partial pressures of about 10^{-3} atmosphere. Hydrogen, because of its narrow linewidth and population distribution, should have a signal-to-noise ratio of 1 at about 10^{-5} atmosphere. Pure gases at low pressure where the linewidth is determined primarily by Doppler broadening, may be detected at pressures several orders of magnitude lower than this. The ultimate detectability depends upon laser power and saturation effects.

Simple relationships have been derived which allow the prediction of the uncertainty in temperature of a gas for an assumed signal-to-noise ratio.

In a plasma the inverse bremsstrahlung process is found to transfer insufficient energy to the plasma to significantly modify the parameters measured.

The experimental attempt at background reduction by interferometric cancellation verified that the principles were correct. Complete cancellation, however, was not observed. This is thought to be due to the diffraction limitations of optical lenses.

One area of additional research and experimentation that could further extend the applications of CARS is that of the background suppression. Another area of improvement needs to

be that of the fluctuating intensities of the high power pulsed lasers that are available.

APPENDIX A

STIMULATED RAMAN SCATTERING

A. DEVELOPMENT

The interaction of two electromagnetic fields in a material is such that different combinations of the two may produce additional fields. The two additional fields of interest here are the Stokes and anti-Stokes frequencies.

Raman scattering has been observed extensively and found to produce the Stokes and anti-Stokes frequencies at plus and minus the vibrational frequency, ω_V , of the molecule from the incident light, ω_I .

$$\omega_{\text{Stokes}} = \omega_I - \omega_V \quad (\text{A1})$$

$$\omega_{\text{anti-Stokes}} = \omega_I + \omega_V \quad (\text{A2})$$

Stimulated Raman scattering predicts a gain in the strength of a field as it traverses a media. The media of interest in this study are gases. The gain will be related to the non-linear susceptibility of those gases.

Beginning with Maxwell's equations, which contain various assumptions implied by their form, the plane wave equation is derived from the curl of the curl of the electric field, E . Assuming a solution to the wave equation of the form:

$$E = \frac{1}{2} (\epsilon e^{-i(kz - \omega t)} + \text{c.c.}) \quad (\text{A3})$$

where ϵ is the amplitude, k is the propagation constant

and ω is the frequency. For simplicity, all fields have been reduced to one dimension along the z axis. From the nonlinear polarization term the various possible frequencies are defined and their field properties (gain or attenuation) are explained by computing the solution to the wave equation. For completeness both MKSA and CGS results are presented.

The development in MKSA units begins with Maxwell's basic and constituent equations.

$$\begin{aligned}\nabla \times \mathbf{H} &= \mathbf{J} + \dot{\mathbf{D}} & \mathbf{D} &= \epsilon_0 \mathbf{E} + \mathbf{P} \\ \nabla \times \mathbf{E} &= -\dot{\mathbf{B}} & \mathbf{J} &= \sigma \mathbf{E} \\ \nabla \cdot \mathbf{E} &= 0 & \mathbf{P} &= \epsilon_0 \chi \mathbf{E} + \mathbf{P}_{NL} \\ \nabla \cdot \mathbf{B} &= 0 & \mathbf{B} &= \mu_0 \mathbf{H}\end{aligned}$$

The curl of \mathbf{H} becomes

$$\nabla \times \mathbf{H} = \sigma \mathbf{E} + \epsilon_0 \dot{\mathbf{E}} + \dot{\mathbf{P}} = \sigma \mathbf{E} + \epsilon \dot{\mathbf{E}} + \dot{\mathbf{P}}_{NL}.$$

Then the wave equation, defined from $\nabla \times (\nabla \times \mathbf{E})$ is

$$-\nabla^2 \mathbf{E} = -\frac{d}{dt} (\nabla \cdot \mathbf{B}) = -\mu_0 \frac{d}{dt} (\nabla \times \mathbf{H})$$

or

$$\ddot{\mathbf{E}} + \frac{\sigma}{\epsilon} \dot{\mathbf{E}} - \frac{\nabla^2 \mathbf{E}}{\mu_0 \epsilon} = -\frac{1}{\epsilon} \ddot{\mathbf{P}}_{NL}. \quad (\text{A4})$$

Using the assumed form of the solution, equation (A3), and the assumptions that $\sigma = 0$ and $\partial^2 \epsilon / \partial z^2$ is very small, then equation (A4) becomes

$$\begin{aligned}
& -\frac{\omega^2}{2} (\epsilon e^{i(kz - \omega t)} + \text{c.c.}) + \frac{k^2 c^2}{2\eta^2} (\epsilon e^{i(kz - \omega t)} + \text{c.c.}) \\
& - \frac{kc^2}{\eta^2} \left[i \frac{\partial \epsilon}{\partial z} e^{i(kz - \omega t)} + \text{c.c.} \right] = - \frac{1}{\epsilon} \ddot{P}_{NL}.
\end{aligned} \tag{A5}$$

The usual definitions:

$$c^2 = \frac{1}{\mu_0 \epsilon_0}$$

$$\eta = \sqrt{\epsilon/\epsilon_0}$$

$$k = \omega \eta/c$$

have also been used.

For the two interactive fields E_1 and E_2 the nonlinear polarization, P_{NL} is expressed as: [18]

$$P_{NL} = 3\epsilon_0 \chi^{(3)} E_1^2 E_2. \tag{A6}$$

Three frequencies are possible from the $E_1^2 E_2$ combination; ω_2 , $2\omega_1 - \omega_2$, $2\omega_1 + \omega_2$. If E_2 is the Stokes field with frequency ω_2 (assuming $\omega_1 < \omega_2$) then a resultant field, E_3 , of frequency $2\omega_1 - \omega_2$ is the anti-Stokes field. For the anti-Stokes calculations P_{NL} is given by:

$$P_{NL} = 3\epsilon_0 \chi^{(3)} \left(\frac{1}{8} \epsilon_1 \epsilon_1 \epsilon_2^* \right) [e^{-i[(2k_1 - k_2)z - (2\omega_1 - \omega_2)t]} + \text{c.c.}]. \tag{A7}$$

The resultant field may be E_2 for the case when

$$P_{NL} = 3\epsilon_0 \chi^{(3)} \left(\frac{1}{8} \epsilon_1 \epsilon_1 \epsilon_2^* \right) [e^{-i(k_2 z - \omega_2 t)} + \text{c.c.}]. \tag{A8}$$

1. Stokes Gain Equation

To solve equation (A5) for the Stokes condition, equation (A8), there are two possible alternatives that lead to a gain equation. One way is to assume that $\partial\epsilon_2/\partial z$ is very small and k_2 is complex such that

$$k_2 = k' + ik''.$$

The imaginary part of k_2 , k'' , is then evaluated as:

$$k'' = \frac{\omega_2^3 \chi'' |E_1^0|^2}{2c\eta}$$

where χ'' is the imaginary part of $\chi^{(3)}$ and E_1^0 is the magnitude of E_1 at $z = 0$.

The observed intensity of E_2 is proportional to the time average of $|E_2|^2$ or

$$|\overline{E_2}|^2 = \frac{1}{2} E E^*$$

where

$$\frac{1}{2} E E^* = \frac{1}{8} (\epsilon_2 e^{ik'z} e^{-k''z} + \epsilon_2^* e^{-k'z} e^{-k''z}) \text{ (c.c.)}$$

Thus, $|\overline{E_2}|$ is proportional to $e^{-2k''z}$. χ'' is a negative quantity [27] and therefore $e^{-2k''z}$ is an exponentially growing function with distance.

The other possible way to solve equation (A5) is to let

$$k_2^2 = \frac{\eta_2^2 \omega_2^2}{c^2}$$

and then solve for $\partial\epsilon_2/\partial z$. The result is that

$$\frac{\partial \epsilon_2}{\partial z} = i \left[\frac{\omega_2}{\eta_2 c} \quad 3(\chi' + i\chi'') \quad |E_1^0|^2 \quad \frac{1}{2}\epsilon_2 \right]$$

and again for χ'' negative there is gain for increasing z .

Both approaches result in an intensity gain coefficient, g , such that

$$I_2 = I_2^0 e^{gz}$$

where I_2^0 is the intensity of I_2 at $z = 0$. The result is that

$$g = \frac{\omega_2}{\eta_2 c} \quad |3\chi''| \quad |E_1^0|^2. \quad (A9)$$

For cgs units the gain is

$$g = \frac{4\pi\omega_2}{\eta_2 c} \quad |3\chi''| \quad |E_1^0|^2. \quad (A10)$$

2. Anti-Stokes Gain Equation

Solving equation (A5) for the anti-Stokes condition (A7) results in the gain equation for the anti-Stokes field. The only way to solve equation (A5) is to assume

$$k_3 = \frac{\eta_3^2 \omega_3^2}{c^2}.$$

The result is that

$$\frac{\partial \epsilon_3}{\partial z} = \frac{i\omega_3}{\eta_3 c} \quad 3(\chi' + i\chi'') \quad \frac{1}{8}\epsilon_1\epsilon_1\epsilon_2^* \quad e^{i\Delta kz} \quad (A11)$$

where $\Delta k = 2k_1 - k_2 - k_3$.

Again if χ'' is negative, there is gain. In cgs units

$$\frac{\partial \epsilon_3}{\partial z (\text{cgs})} = 4\pi \left(\frac{\partial \epsilon_3}{\partial z} \right)_{\text{MKSA}}. \quad (\text{A12})$$

B. CORRELATION OF VARIOUS ARTICLES

The only published values for nonresonant susceptibilities of gases are those given by Rado [21]. It was desirable to check for consistency in the equations used by Rado and the ones used to calculate resonant susceptibilities.

The basis for Rado's experimental values of χ_{NR} was the resonant value of $\chi^{(3)}$ for H_2 from other experimental data [23]. The gain coefficient for Stokes Stimulated Raman Scattering provided Rado with the needed value of χ_{R} for H_2 at pressures greater than 10 atmospheres. The gain coefficient was given in [28] in cgs units as

$$\frac{g}{I_1} = \frac{k[8\pi^2 L \Delta N \alpha^2] \tau_r}{\epsilon c \eta \hbar} \times 10^7 \text{ (cm/W)} \quad (\text{A13})$$

where L is the local field correction factor, N is the number density of atoms, Δ is the population ratio, τ_r is the phonon lifetime, α is the polarization coefficient and I_1 is the incident laser intensity.

An independent article by Maier [29] used the following definition for the gain coefficient

$$\frac{g}{I_1} = \frac{8\pi N \omega \alpha^2}{\hbar \eta^2 c^3 \Delta \nu}$$

where $\Delta \nu$ is a linewidth. Rado's gain is equivalent to Maier's if

$$\Delta = 1.$$

$$L = 1.$$

$$\epsilon = \eta^2$$

and

$$\tau_r = 1/2\pi c \Delta\nu.$$

The experimentally observed gain for H_2 above 10 atmospheres was stated as 1.45×10^{-9} cm/W for an incident light source of 975 nm. If the gain coefficient developed in equation (A10) is divided through by intensity then

$$\frac{g}{I_1} = \frac{32\pi^2 \omega_2 |3\chi''|}{c^2 \eta^2}. \quad (A15)$$

Solving for $|3\chi''|$ the result is

$$|3\chi''| = \frac{gc\lambda_2}{64\pi^3} \quad (A16)$$

assuming $\eta^2 = 1$. The value for $3\chi''$ is the same as that used by Rado to represent χ'' .

The gain coefficients given in two textbooks more nearly resemble the gain coefficient in equation (A9). Pantell and Putoff [30] define g in MKS units as

$$g = \frac{4\pi \chi'' I_1}{\lambda_2 \eta_2 \eta_1 \epsilon_0 c} \quad (A17)$$

whereas equation (9) may be rearranged as

$$g = \frac{4\pi |3\chi''| I_1}{\lambda_2 \eta_2 \epsilon_0 c} \quad (A18)$$

differing from Pantell by a factor of η_1 . If $\eta_1 = 1$, they

become the same. Yariv [27] gives a voltage gain coefficient as

$$g' = \frac{k_2}{2\eta_2} |E|^2 |\chi''|. \quad (\text{A19})$$

The intensity gain, g , would be $2g'$. Thus, the intensity gain coefficient is

$$2g' = g = \frac{k_2}{\eta_2} |E|^2 |\chi''| = \frac{\omega_2}{\eta_2 c} |\chi''| |E|^2. \quad (\text{A20})$$

PROGRAM TO CALCULATE THE LOCAL PEAK VALUES OF THE
 RESONANT THIRD-ORDER NONLINEAR DIELECTRIC
 SUSCEPTIBILITY,CHI, FOR A DIATOMIC GAS

THE PROGRAM HAS THE NECESSARY CONSTANTS
 INTERNALLY TO CALCULATE CHI FOR
 OXYGEN,NITROGEN,HYDROGEN AND CARBON MONOXIDE.

EACH GAS HAS AN IDENTIFIER (G).

GAS	CODE(G)
OXYGEN	1
NITROGEN	2
HYDROGEN	3
CARBON MONOXIDE	4

THE REQUIRED INPUT FOR A CALCULATION IS

TEMPERATURE(T) IN DEGREES KELVIN
 PRESSURE(P) IN ATMOSPHERES
 LINEWIDTH(GAMA) IN INVERSE CM (1/CM)
 GAS IDENTIFIER CODE (G)
 A TEMPERATURE OF 0. STOPS THE PROGRAM

THE INTERNAL DATA CONSISTS OF

DSIG: THE TOTAL RAMAN CROSS SECTION
 WV: THE MOLECULAR VIBRATIONAL FREQUENCY(1/CM)
 B: THE ROTATIONAL CONSTANT(1/CM)
 RI: SPIN OF EACH NUCLEI
 ALPH: THE ROTATION-VIBRATIONAL INTERACTION TERM
 FREGE: HARMONIC VIBRATIONAL FREQUENCY(1/CM)
 XE: ANHARMONIC CONSTANT TIMES FRECE (1/CM)
 WINC: THE DIFFERENCE FREQUENCY INCREMENT(1/CM)

```

CCCC
      CCMPLEX DENOM
      REAL CHIMAX(60),WMAX(60)
      REAL GP(9,10),ZJ(60),FREQJ(60),WI(3),CARS(3),GJ(61)
      INTEGER
      DATA GP/1,2,0034,1,556E03,1,44567,0,0,01575,1580,261,12,073,001,
21,00055,2330,7,1,5987,1,0,01781,2358,07,14,188,001,
31,00234,155E03,60,864,5,3,07638,4400,35,120,815,005,
41,00055,2,143E03,1,93127,99,0,017513,2165,823,13,2539,001,54*1,
100 FCFRMT(3,F5,0,12)
200 FCFRMT(1X,E15,8,F10,3)
300 FCFRMT(1X,LINEWN AT ,F5,0, DEGREES K')
500 FCFRMT(1X,OXYGEN AT ,F5,0, DEGREES K')
510 FCFRMT(1X,NITROGEN AT ,F5,0, DEGREES K')
520 FCFRMT(1X,HYDROGEN AT ,F5,0, DEGREES K')
530 FCFRMT(1X,CO AT ,F5,0, DEGREES K')
540 FCFRMT(1X, FOR ,F5,0, ATOMS PRESSURE)
700 FCFRMT(1X,///)

C**REAC THE INPUT VARIABLES
C
30C REAL(5,100)T,P,GAMA,G
      WRITE(6,700)
      IF(G.EQ.1)WRITE(6,510)T
      IF(G.EQ.2)WRITE(6,520)T
      IF(G.EQ.3)WRITE(6,530)T
      IF(G.EQ.4)WRITE(6,540)T
      IF(T.EQ.0.) STOP
      N=0

C**INITIALIZE THE NUCLEAR SPIN WEIGHTING FACTOR MATRIX(GJ)
C
      CC 6 L=1,61
      C GJ(L)=1.

C**PULL THE REQUIRED DATA FROM THE DATA MATRIX(GP)
C
      CSIG=GP(1,G)
      WV=GP(3,G)
      B=GP(4,G)
      RI=GP(5,G)
      ALFH=GP(6,G)
      AFCE=GF(7,G)
      XE=GP(8,G)
      WINC=GP(9,G)

```

CH100010
 CH100020
 CH100030
 CH100040
 CH100050
 CH100060
 CH100070
 CH100080
 CH100090

CH100120
 CH100130
 CH100140
 CH100150
 CH100160
 CH100170
 CH100180

CH100190
 CH100200
 CH100210
 CH100220
 CH100230
 CH100240
 CH100260
 CH100250

CH100270
 CH100280

CH100290
 CH100300
 CH100310
 CH100320
 CH100330
 CH100340
 CH100350
 CH100360


```

C**CALCULATE THE PARTITION FUNCTION Z
C
C 2 Z=Z+ZJ(L)*GJ(L)
C**BEGIN THE CALCULATIONS .1 1/CM FROM THE FIRST FREQUENCY
C
C 7 W=FREQJ(1)+.1
CARS(1)=0.
CARS(2)=0.
CARS(3)=0.
C**BEGIN CALCULATING CHI
C
C 3 K=1,6000
W=W+WINC
C 1=0.
C 4 L=1,60
CENCM=CMPLX(FREQJ(L)**2-W*W,GAMA*W*(-1.))
CHIJ=P*DSIG*ZJ(L)*GJ(L)*FREQJ(L)*4.90E-14*(1.-EXP(WV*(-1.4404)/
1T))*2/(T*Z*SQR(TREAL(DENOM*CONJG(DENOM))))
C 4 CHI=CHI+CHIJ
CCONTINUE
C 1(1)=W+2.*WINC
W1(2)=W+WINC
W1(3)=W
CARS(1)=CARS(2)
CARS(2)=CARS(3)
CARS(3)=CHI
IF(CARS(2).GT.CARS(1).AND.CARS(3).LE.CARS(2)) GO TO 8
C 3
C 8 N=N+1
C**DETERMINE THE PEAK VALUE BY A THREE PCINT PARAEGLIC FIT
C
C 3 CHIMAX(N)=(5./8.)*(CARS(1)-CARS(2))*2/(CARS(1)+CARS(3))+CARS(2)
C**DETERMINE THE CORRESPONDING FREQUENCY
C
C WMAX(N)=.5*(CARS(1)-CARS(3))/(CARS(1)+CARS(3))+WI(2)
WRITE(6,200)CHIMAX(N),WMAX(N)
CCONTINUE
C 3
C 300
ENC

```

CHI00580

CHI00590
CHI00600
CHI00610
CHI00620

CHI00630
CHI00640
CHI00650
CHI00660
CHI00670
CHI00680
CHI00690
CHI00700
CHI00730
CHI00740
CHI00750
CHI00760
CHI00770
CHI00780
CHI00790
CHI00800
CHI00810
CHI00820

CHI00830

CHI00840
CHI00850
CHI00870
CHI01110

PROGRAM TO CALCULATE THE UNCERTAINTY IN A
 TEMPERATURE MEASUREMENT BASED ON THE CHANGE
 IN CHI SQUARED WITH RESPECT TO TEMPERATURE
 THE PROGRAM HAS THE NECESSARY CONSTANTS
 INTERNALLY TO CALCULATE CHI FOR
 OXYGEN, NITROGEN, HYDROGEN AND CARBON MONOXIDE.

EACH GAS HAS AN IDENTIFIER (G).

GAS	CODE (G)
OXYGEN	1
NITROGEN	2
HYDROGEN	3
CARBON MONOXIDE	4

THE REQUIRED INPUT FOR A CALCULATION IS

TEMPERATURE(T) IN DEGREES KELVIN
 PRESSURE(P) IN ATMOSPHERES
 LINEWIDTH(GAMA) IN INVERSE CM (1/CM)
 GAS IDENTIFIER CODE (G)
 A TEMPERATURE OF 0. STOPS THE PROGRAM

THE INTERNAL DATA CONSISTS OF

DSIG: THE TOTAL RAMAN CROSS SECTION
 WV: THE MOLECULAR VIBRATIONAL FREQUENCY(1/CM)
 B: THE ROTATIONAL CONSTANT(1/CM)
 RI: SPIN OF EACH NUCLEI
 ALPH: THE ROTATION-VIBRATION INTERACTION TERM
 FREQ: THE HARMONIC VIBRATIONAL FREQUENCY(1/CM)
 XE: ANHARMONIC CONSTANT TIMES FREQUENCY(1/CM)
 WINC: THE DIFFERENCE FREQUENCY INCREMENT(1/CM)

CCCC

```

CCOMPLEX DENGIM
REAL CHIMAX(120),WMAX(120)
REAL GP(9,10),ZJ(60),FREQJ(60),W(3),CARS(3),GJ(61),CHISAV(2,16000)
1) INTEGER G
DATA GP/1.2, .0034, 1.556E03, 1.44567, 0., .01579, 1580.361, 12.073, .001,
21.0, .0055, 2330.7, 1.9987, 1., .01781, 2358.07, 14.188, .001,
31.0, .03, 4.155E03, 60.864, 5, 3.07638, 4400.35, 120.815, .005,
41.2, .005, 2.143E03, 1.93127, 99., .017513, 2169.623, 13.2939, .005, 54*1.
1)
100 FCFMAT(3F5.0, I2)
1200 FCFMAT(1X, I3, E15.8, F10.3)
400 FCFMAT(1X, I3, E15.8)
500 FCFMAT(1X, LINEWIDTH, USED, F10.4) DEGREES K.)
510 FCFMAT(1X, OXYGEN AT, F5.0, DEGREES K.)
520 FCFMAT(1X, NITROGEN AT, F5.0, DEGREES K.)
530 FCFMAT(1X, HYDROGEN AT, F5.0, DEGREES K.)
540 FCFMAT(1X, CO AT FOR, F5.0, ATOMS PRESSURE)
600 FCFMAT(1X, ///)
700 FCFMAT(1X, DCHI-DT SQUARED AND SUMMED =, F15.8)
800 FCFMAT(1X, SIGMA T =, F10.1, DEGREES K.)
810 FCFMAT(1X, TO FIND DCHI-DT)
900 FCFMAT(1X, TO FIND DCHI-DT)

```

C**FEAC THE INPUT VARIABLES

```

300 REAL(5, 100)T, P, GAMMA, G
WRITE(6, 700)
IF(G.EQ.1)WRITE(6, 510)T
IF(G.EQ.2)WRITE(6, 520)T
IF(G.EQ.3)WRITE(6, 530)T
IF(G.EQ.4)WRITE(6, 540)T
N=0
N=1
CC 15 KK=1, 2
IF(T.EQ.0.)} STOP

```

C**INITIALIZE THE SPIN WEIGHTING FACTOR MATRIX(GJ)

```

CC 6 L=1, 61
C GJ(L)=1.

```

C**FULL THE REQUIRED DATA FROM THE MATRIX(GP)

CHI00360
CHI00370
CHI00380
CHI00390
CHI00400
CHI00410
CHI00420
CHI00430

CHI00440

CHI00450
CHI00460
CHI00470
CHI00480
CHI00490
CHI00500

CHI00510
CHI00520

CHI00530
CHI00540
CHI00550
CHI00560
CHI00570
CHI00580

CHI00590

CHI00600

```

C      CSIG=GP(1,G)
C      WV=GP(3,G)
C      P=GP(4,G)
C      R1=GP(5,G)
C      ALFT=GP(6,G)
C      FREQE=GP(7,G)
C      XE=GP(8,G)
C      WINC=GP(9,G)

C**LINEWIDTH (GAMA) MAY BE STCRED IN GP(2,G)
C
C**DETERMINE THE WEIGHTING FACTOR(GJ) FOR EACH ROTATIONAL J
C
C      JJ=1
C      F=RI/(RI+1.)
C      IF(RI.EQ.99.) F=1.
C      I=RI*2
C      WRITE(6,500)GAMA
C      WRITE(6,600)P

C**START WITH F IN THE CCD J POSITIONS -
C
C      CC 1 L=2,60,2
C      1 GJ(L)=F

C**DETERMINE IF RI IS A WHOLE OR HALF INTEGER
C**HALF INTEGER JJ=1
C**WHOLE INTEGER JJ=0
C
C      IF((I-(I/2)*2).LT..5) JJ=0
C      CC 5 L=1,60
C
C      J=L-1
C      JJ=JJ+1
C      GJ(L)=GJ(JJ)

C**CALCULATE THE ROTATIONAL FREQUENCIES
C
C      FFECJ(L)=FREQE-(ALPH*J*L)-(2.*XE)

C**INITIALIZE THE POPULATION OF EACH LEVEL TO 0
C
C      ZJ(L)=0.

C**ASSUME A BOLTZMAN DISTRIBUTION FOR EACH LEVEL
C

```

```

      CC 2 L=1,60
      J=L-1
      ZJ(L)=((2.*J)+1.)*EXP(J*L*(-1.4404)*B/T)
C**ASSUME NO POPULATION FOR SMALL VALUES OF ZJ
C
      IF(ZJ(L).LT.1.E-5) GO TO 7
C**CALCULATE THE PARTITION FUNCTION Z
C
      2 Z=Z+ZJ(L)*GJ(L)
C**BEGIN THE CALCULATIONS .1 1/CM FROM THE FIRST FREQUENCY
C
      7 W=FREQJ(1)+.1
      CARS(1)=0.
      CARS(2)=0.
      CARS(3)=0.
C**BEGIN CALCULATING CHI
C
      CC 3 K=1,16000
      W=W-WINC
      CHI=0.
      CC 4 L=1,60
      DENOM=CMPLX(FREQJ(L)**2-W*W,GAMA*W*(-1.))
      CHIJ= P*CSIG*ZJ(L)*GJ(L)*FREQJ(L)*4.90E-14*(1.-EXP(W*W*(-1.4404)/
      1T))**2/(T*Z*SQRT(REAL(DENOM*CONJG(DENOM))))
      CHI=CHI+CHIJ
C**SQUARE AND SAVE ALL VALUES CALCULATED
C
      CHI=ISAV(M,K)=CHI*CHI
      4 CCNTINUE
      W1(1)=W+2.*WINC
      W1(2)= W+WINC
      W1(3)=W
      CARS(1)=CARS(2)
      CARS(2)=CARS(3)
      CARS(3)=CHI
      IF(CARS(2).GT.CARS(1).AND.CARS(2).LE.CARS(3)) GO TO 8
      CC TO 3
      5 N=N+1
C**CALCULATE THE MAXIMUM VALUES OF CHI BY A THREE FCINT FIT
C
      CFIMAX(N)=(5./8.)*(CARS(1)-CARS(3))**2/(CARS(1)+CARS(3))+CARS(2)
      WMAX(N)=.5*(CARS(1)-CARS(3))/(CARS(1)+CARS(3))+WI(2)

```

CHI00610
CHI00620
CHI00630

CHI00640

CHI00650

CHI00660
CHI00670
CHI00680
CHI00690

CHI00700
CHI00710
CHI00720
CHI00730
CHI00740
CHI00750
CHI00760
CHI00770

CHI00780
CHI00790
CHI00800
CHI00810
CHI00820
CHI00830
CHI00840
CHI00850
CHI00860
CHI00870
CHI00880

CHI00890
CHI00900

CHI00910

CHI00920
CHI00930
CHI00940

CHI00950
CHI00960
CHI00970
CHI00980
CHI00990
CHI01000
CHI01010
CHI01020
CHI01030
CHI01040
CHI01050
CHI01060
CHI01070
CHI01080

CHI01090
CHI01100

CHI01110
CHI01120
CHI01130
CHI01140
CHI01150

```

3 CCNTINUE
C**INCREMENT THE TEMPERATURE BY ONE DEGREE THEN CALCULATE
C ALL THE VALUES OF CHI AGAIN
C
  T=T+1.
  M=2
15 CCNTINUE
C**DETERMINE THE PEAK VALUE OF THE LOCAL PEAKS
C FOR T AND T+1
C
  N2=N/2
  SCALE1=0.
  CC 12 JJ=1,N2
  IF (CHIMAX(JJ)**2.GE.SCALE1) SCALE1=CHIMAX(JJ)**2
12 CCNTINUE
  N2F1=N2+1
  SCALE2=0.
  CC 13 J=N2P1,N
  IF (CHIMAX(J)**2.GE.SCALE2) SCALE2=CHIMAX(J)**2
13 CCNTINUE
  SIGMA=0.
  CC 16 K=1,16000
C** DETERMINE THE DIFFERENCE IN CHI SQAURED AND SUM LP
C
  SIGMA=SIGMA+((CHISAV(1,K)/SCALE1)-(CHISAV(2,K)/SCALE2))**2
16 CCNTINUE
C**EF IS THE UNCERTAINTY IN THE INTENSITY OF THE MCST
C INTENSE SPECTRAL LINE
C
  EF=.1
  SIGMAT=EF/SQRT(SIGMA)
  WRITE(6,810)SIGMAT
  GC TO 300
  ENC
C
C
C
C
```


LIST OF REFERENCES

1. Levenson, M. D.; Flytzanis, C.; and Bloembergen, N.; "Interference of Resonant and Nonresonant Three-Wave Mixing in Diamond," Physical Review B, v. 6, p. 3962-3966, 15 November 1972.
2. Wynne, J. J., "Nonlinear Optical Spectroscopy of $\chi^{(3)}$ in LiNbO_3 ," Physical Review Letters, v. 29, p. 650-653, 4 September 1972.
3. Yablonovitch, E.; Flytzanis, C.; and Bloembergen, N.; "Anisotropic Interference of Three Wave and Double Two-Wave Frequency Mixing in GaAs," Physical Review Letters, v. 29, p. 865-867, 25 September 1972.
4. Régnier, P. R. and Taran, J. P. E., "On the Possibility of Measuring Gas Concentrations by Stimulated Anti-Stokes Scattering," Applied Physics Letters, v. 23, p. 240-242, 1 September 1973.
5. Levenson, M. D. and Bloembergen, N., "Dispersion of the Nonlinear Optical Susceptibility Tensor in Centrosymmetric Media," Physical Review B, v. 10, p. 4447-4463, 15 November 1974.
6. Levenson, M. D. and Bloembergen, N., "Dispersion of the Nonlinear Optical Susceptibilities of Organic Liquids and Solutions," The Journal of Chemical Physics, v. 60, p. 1323-1327, 15 February 1974.
7. DeMartini, F.; Givliana, G. P.; and Santamato, E.; "Line Profile of the $Q_{01}^{(1)}$ Vibrational Resonance in H_2 in the Zone of Dicke Narrowing," Optics Communications, v. 5, p. 126-130, May 1972.
8. Nabara, A. and Kubota, K., "Three-Wave Optical-Mixing Effects in Wedge-Shaped Cells," Japanese Journal of Applied Physics, v. 6, p. 1105-1108, September 1967.
9. Régnier, P. R.; Moya, F.; and Taran, J. P. E.; "Gas Concentration Measurements by Coherent Raman Anti-Stokes Scattering," AIAA Journal, v. 12, p. 826-831, 1974.
10. Itzkan, I. and Leonard, D. A., "Observation of Coherent Anti-Stokes Raman Scattering from Liquid Water," Applied Physics Letters, v. 26, p. 106, 1975.
11. Moya, F.; Druet, S. A. J.; and Taran, J. P. E.; "Gas Spectroscopy and Temperature Measurement by Coherent Raman Anti-Stokes Scattering," Optics Communications, v. 13, p. 169, 1975.

12. Klauminzer, G., "CARS Improved Experimental Design and Observation of New HORSES," Applied Physics Letters, v. 28, January 1976.
13. Barrett, J. J. and Begley, R. F., "Low-Power CW Generation of Coherent Anti-Stokes Raman Radiation in CH₄ Gas," Applied Physics Letters, v. 27, p. 129-131, 1975.
14. Moya, F.; Druet, S.; Péalat, M.; and Taran, J. P.; "Flame Investigation by Coherent Anti-Stokes Raman Scattering," AIAA Paper No. 76-29, presented at the AIAA 14th Aerospace Sciences Meeting and 12th Annual Meeting Aerospace 1976, Washington, D. C., January 26-30, 1976.
15. Maker, P. D. and Terhune, R. W., "Study of Optical Effects Due to an Induced Polarization Third Order in the Electric Field Strength," Physical Review, v. 137, p. A801-A818, 1 February 1965.
16. Tolles, W. M. and Turner, R. D., "A Comparative Analysis of the Analytical Capabilities of Coherent Anti-Stokes Raman Spectroscopy Relative to Raman Scattering and Absorption Spectroscopy," unpublished, submitted to Applied Spectroscopy, May 1976.
17. Yablonovitch, E.; Bloembergen, N.; and Wynn, J. J.; "Dispersion of the Nonlinear Optical Susceptibility in n-Insb," Physics Review B, v. 3, p. 2060, 1971.
18. Naval Research Laboratory (NRL) Memorandum Report 3260, Theoretical Development of Third-Order Susceptibility as Related to Coherent Anti-Stokes Raman Spectroscopy (CARS), by R. N. DeWitt, A. B. Harvey and W. M. Tolles, p. 6, 7, 35, B5, April 1976.
19. Chang, R. K. and Fouche, D. G., "Gains in Detecting Pollution," Laser Focus, p. 43-45, December 1972.
20. Bloembergen, N., Nonlinear Optics, p. 7, W. A. Benjamin, Inc., 1965.
21. Rado, W. G., "The Nonlinear Third-Order Dielectric Susceptibility Coefficient of Gases and Optical Third Harmonic Generation," Applied Physics Letters, v. 11, p. 123-124, 15 August 1967.
22. Young, H. D., Statistical Treatment of Experimental Data, McGraw-Hill, 1962.
23. Lochte-Holtgreven, W., editor, Plasma Diagnostics, p. 589, North-Holland, 1968.
24. Chen, F. F., Introduction to Plasma Physics, p. 37, Plenum Press, 1974.

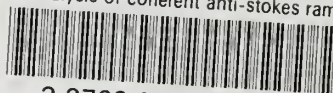
25. Spitzer, L., Jr., Physics of Fully Ionized GASES, p. 80, 89, Interscience Publishers, 1956.
26. Tolles, W. M., personal conversation.
27. Yariv, A., Quantum Electronics, 2nd ed., p. 487, John Wiley & Sons, 1975.
28. Hagenlocker, E. E.; Minck, R. W.; and Rado, W. G.; "Effects of Phonon Lifetime on Stimulated Optical Scattering in Gases," Physical Review, v. 154, p. 226-233, 10 February 1967.
29. Maier, M.; Kaiser, W.; and Giordmaine, J. A.; "Backward Stimulated Raman Scattering," Physics Review, v. 177, p. 580, 1969.
30. Pantell, R. H. and Puthoff, H. E., Fundamentals of Quantum Electronics, p. 60, 235, John Wiley & Sons, 1969.

INITIAL DISTRIBUTION LIST

	No. Copies
1. Defense Documentation Center Cameron Station Alexandria, Virginia 22314	2
2. Library, Code 0212 Naval Postgraduate School Monterey, California 93940	2
3. Department Chairman, Code 61 Department of Physics and Chemistry Naval Postgraduate School Monterey, California 93940	2
4. Professor W. M. Tolles, Code 61T1 Department of Physics and Chemistry Naval Postgraduate School Monterey, California 93940	4
5. LT Ronald D. Turner, USN 329 Farrell Street Norfolk, Virginia 23503	1

thesT9565

An analysis of coherent anti-stokes rama



3 2768 001 88903 3

DUDLEY KNOX LIBRARY